ce/papers
The online collection for conference papers in civil engineering
Ernst & Sohn A Wiley Brand

ORIGINAL ARTICLE

eurosteel SHEFFIELD 2021
Ernst & Sohn A Wiley Brand

Modified strut and tie model of headed stud shear connectors in open trough profiled sheeting for predicting the post-cracking load bearing resistance

Valentino Vigneri[1], Christoph Odenbreit[1], Dennis Lam[2], François Hanus[3]

Correspondence

Valentino Vigneri
University of Luxembourg
Faculty of Science, Technology & Medicine
Rue Richard Coudenhove-Kalergi 6
Luxembourg
Email: valentino.vigneri@uni.lu

Affiliations

[1]University of Luxembourg, Luxembourg, Luxembourg.
[2]University of Bradford, Bradford, UK
[3]ArcelorMittal Steligence®, Luxembourg, Luxembourg

Abstract

Current EN 1994-1-1 provides statistically calibrated equations for predicting the strength of headed stud shear connectors in profiled steel sheeting. Recent tests showed that the design resistance is overestimated for some novel open trough decks. A mechanical model was developed within the RFCS Project DISCCO [3] that considers "stud in bending" component and the elastic bending resistance of the concrete rib separately (1-2 mm slip). However, to represent the behaviour of the connector in the post-cracking stage (2-6 mm), a "Modified Strut and Tie" model was developed with the support of experimental and numerical results. The concrete and the steel deck were replaced by a system of strut and tie elements whereas the stud was considered as a beam with one or two plastic hinges. In accordance with test observations, the authors assumed that the resistance of the model is limited by the capacity of the strut in front of the stud estimated through an analogy with RC corbels. The analytical resistance of the system was finally derived and compared with the results of 193 push-out tests: the statistical evaluation delivered a correlation coefficient of 0.81 and a coefficient of variation of 0.15.

Keywords

Headed stud, Shear connector, Strut and Tie model, Mechanical model, Analytical equations

1 Introduction

Composite steel-concrete composite structures combine the compressive resistance of the concrete with the tensile strength and deformation capacity of the structural steel. One of the typical steel-concrete building applications consist of a I-section steel beam supporting a composite reinforced concrete slab with profiled steel sheeting. The steel deck acts as a formwork in the construction stage whereas it provides good structural performance in bending. Such solution is economically efficient and it is one of the most popular in the modern composite industry. To ensure the composite action of the steel beam and the concrete slab, headed stud shear connectors are generally used at their interface. Such connectors exhibit a good strength and a ductile behaviour that may allow the use of plastic design. Current EN 1994-1-1 [1] provides design rules to predict the load-bearing capacity of headed studs in solid slabs and steel sheeting, parallel and transverse to the supporting beam. In the latter case, the strength is equal to the corresponding resistance of the stud placed in solid slabs multiplied by a reduction factor k_t.

Despite the ease of use, these equations are not able to account for the real mechanical behaviour and the failure modes of the headed studs in steel decking. Based on the push-out test results in the last 20 years [2, 3, 4], it has been found out that the application of current EN 1994-1-1 may lead to unconservative predictions of the shear resistance of headed studs in open trough sheeting [5, 6]. This discrepancy becomes more important when the embedment length of the stud is relatively small or the deck has narrow ribs. Unlike in solid slabs, headed stud shear connectors placed in profiled steel sheeting exhibit a combination of "concrete cone" and "stud in bending" failure leading to concrete pull-out. This type of failure may represent one of the reasons behind the overestimation of the design resistance according to EN 1994-1-1. To properly address this issue, a deep understanding of the mechanical behaviour and the resistance mechanisms involved is necessary, especially at low displacements (within 6 mm slip). As shown in a recent study carried out by the authors [7], the main resistance mechanisms have been identified at different displacements through a complex system of concrete struts.

Several "strut and tie" models were already proposed for predicting the resistance of the studs related to rib punch- through or concrete pull-out failure [8, 9, 10, 11] where the studs carry only tensile forces.

The current manuscript presents an innovative "modified strut and tie" that accounts for the bending component of the stud. The objective is to accurately predict the post-cracking resistance (i.e. after the crack initiation of the concrete cone) of headed stud shear connectors in profiled steel sheeting transverse to the beam. An analogy with the "strut and tie" model used for the shear strength of RC corbel [12, 13] was considered to estimate the resistance of the strut in the rib: such condition reproduces the rib punch-through failure. Additional assumptions and simplifications were made in accordance with experimental and numerically obtained results. Finally, the resulting proposed equation is compared with a database of around 200 push-out test results.

2 Damage pattern and "modified strut and tie model"

Based on new experimental outcomes and the observations of the crack pattern in the concrete rib, the sequence of resistance mechanisms activated in the concrete rib and the headed stud at low slips (1-6 mm) is detailed in this section.

First, due to the high bending stiffness of the concrete rib, the crack starts to develop from the edge of the rib. This is confirmed by recent push-out tests where the specimen was cut after stopping the test at around 2 mm slip, see Figure 1. In parallel, the stud deforms in bending developing one plastic hinge at the bottom. A second upper hinge may be partially or fully activated (not visible from test at small displacements) depending on the geometry of the system [14] [15]. Therefore, at this stage, the resistance of the shear connector P_1 is related to the "concrete cone resistance" and to the bending resistance of the stud. The corresponding mechanical model was presented [5, 6] and the relative design resistance equations were proposed by CEN/TC250/SC4.PT3 to be included in the revised version of EN 1994-1-1.

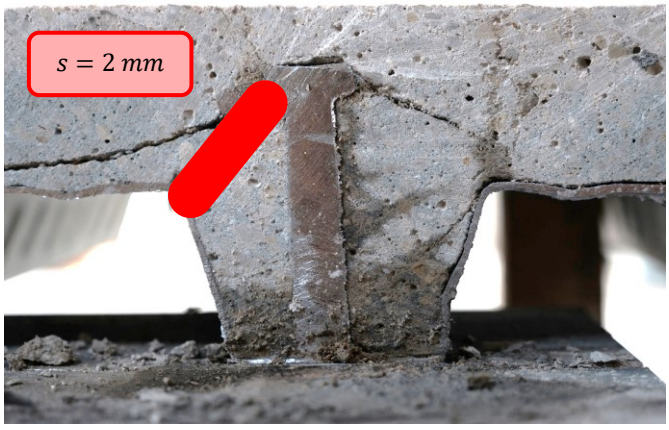

Figure 1 Concrete damage observed in the concrete rib after cutting a push-out test specimen at a slip displacement of 2 mm.

While increasing the slip, the crack further propagates. This leads to the observed concrete cone failure surface shown in Figure 2, where the slip of the shear connector is approximately 6 mm and the concrete cone crack path is fully developed. The resulting "post-cracking" resistance of the connector P_2 is mainly governed by the compressive resistance of the portion of the rib in front of the stud leading to the "rib punch-through" failure. As a result of the progressive crushing of the concrete, the upper hinge moves up towards the head of the stud [15].

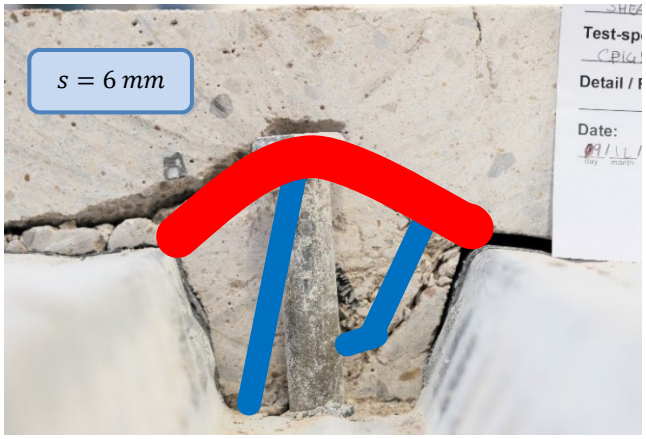

Figure 2 Concrete damage observed in the concrete rib after cutting a push-out test specimen at a slip displacement of 6 mm.

Since headed studs have a ductile behaviour, the resistance values P_1 (at 1-2 mm slip) and P_2 (4-6 mm) are not significantly different. As shown by the typical load-slip curve in Figure 3, the two resistances are generally comparable.

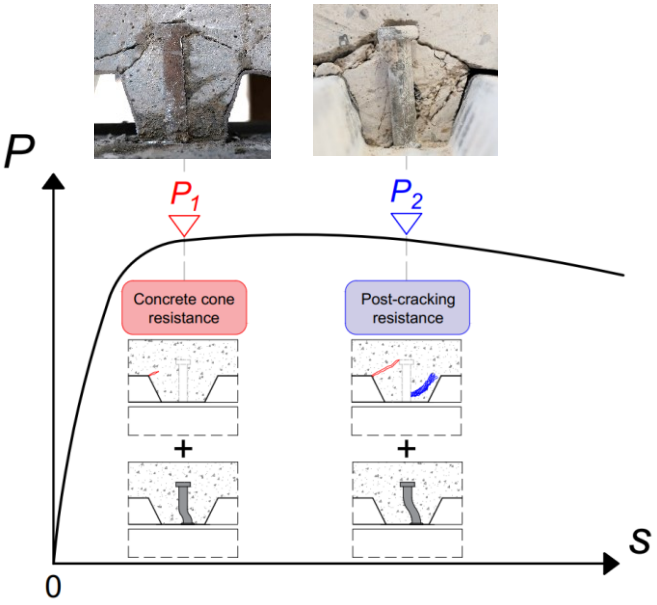

Figure 3 Typical load-slip curve of headed stud shear connector in push-out tests including the "concrete cone" resistance P_1 and the post-cracking resistance P_2

In addition to the experimental outcomes shown in Figure 1 and Figure 2, a validated 3D finite element model of push-out test specimens was used to estimate the position and inclination of the struts [15]. Several numerical simulations were carried out and the distribution of the principal compressive stresses in the concrete is displayed in Figure 4 at a slip of 6 mm.

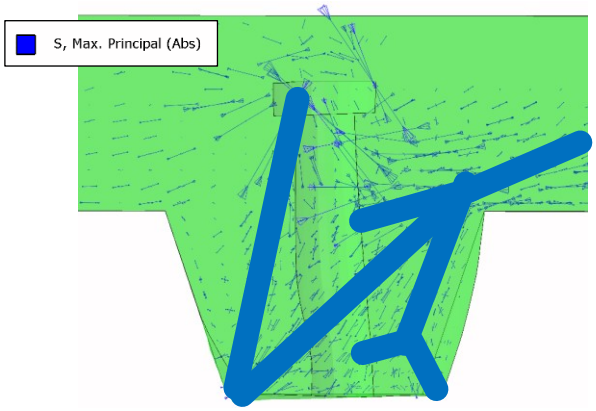

Figure 4 Distribution of the maximum principal compressive stress in the concrete rib from the FE model at a slip of around 6 mm.

The geometry of the "modified strut and tie model" is defined and illustrated in Figure 5. The position of the elements is in agreement with experimental and numerically obtained results. Specifically:

- The struts C_1, C_{11} , C_{12}, replace the behaviour of the concrete in front of the stud. The orientation of the struts C_1 and C_{11} follows the direction of the crack path due to local concrete crushing in Figure 2 and the principal compressive stresses observed in the FE model (Figure 4). The strut C_{12} transfers part of the shear force to the steel sheeting which is able to transfer the load through the tension ties. T_1 and T_3;
- C_3 represents the component of the shear resistance given by the whole rib;
- C_4 replaces the compressive stresses in the concrete that prevent the rotation of the whole connector. A small crack along the direction of the strut C_4 can be also observed in Figure 2;
- C_5 transfers the longitudinal shear force P from the slab to the shear connector. The vertical component of C_5 replicates the vertical shear taken by the slab;
- T_2 accounts for the pulling force of the steel sheeting acting on the stud. (especially in case of through-deck welded studs).

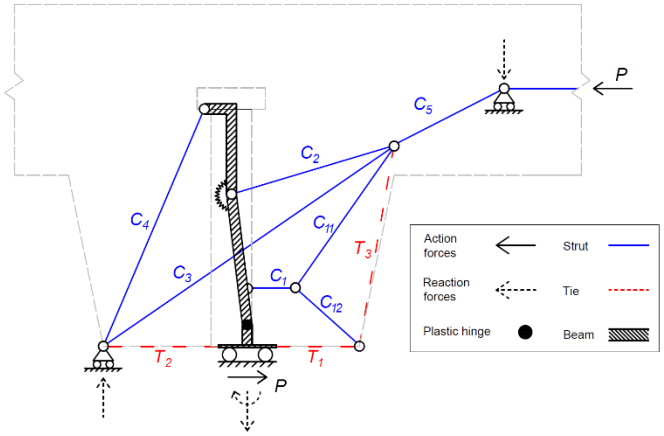

Figure 5 Modified strut and tie model of the headed stud shear connector in standard push-out tests.

3 Derivation of analytical resistance function

3.1 Structural analysis and assumptions

The model presented consists in a planar frame where: the concrete struts replicate the compression stresses in the concrete, the tie elements represent the steel sheeting in tension and the stud is modelled through beam elements. All the key geometric dimensions needed to solve the simplified analytical system are indicated in Figure 6. As observed in the FE model and other numerical studies [16], the bearing forces acting on the stud in profiled sheeting decrease approximately linearly along the height. Assuming a linear distribution of the bearing forces up to the position of the upper hinge with vertical coordinate h_s, the resultant force C_1 applies at a height of $h_s/3$. While the position of the upper plastic hinge was arbitrarily taken as h_s, the lower plastic hinge (at node B) is fixed at a distance $0.5d$ from the steel flange [6].

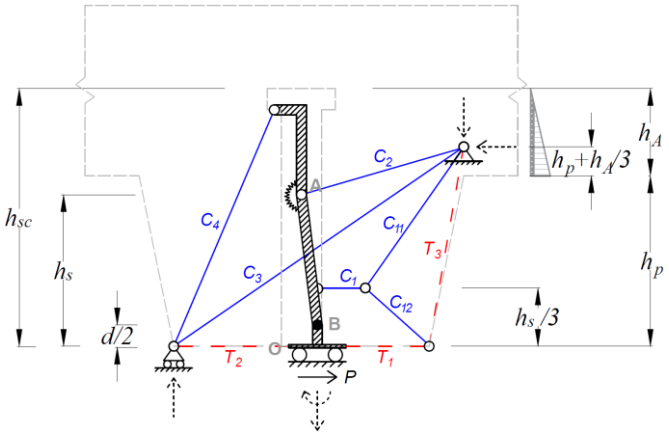

Figure 6 Modified strut and tie model of the headed stud shear connector including the key geometrical dimensions.

The three external equilibrium equations may not be sufficient to calculate all the reaction forces. To assess whether the model is statically determined, the degree of statical indeterminacy n_s shall be calculated and it is given by:

$$n_s = \sum r_i - 3n \tag{1}$$

Where:

n is the number of members

r_i is the number of the restraints of the joint at node i

The total number of members is 12 while the external restraints are 5. If the system in Figure 6 is in the elastic stage (i.e. no plastic hinges) the overall number of internal restraints is 34. By substituting these values in Eq. (1), the degree of statical indeterminacy is given by:

$$n_{s,el} = (5 + 34) - 3 \cdot 12 = 3 \tag{2}$$

Therefore, the system is three times statically indeterminate and it cannot be solved through equilibrium equations. However, when the load increases, the bending moment of the stud at node A reaches the cross-sectional plastic bending resistance. As mentioned in section 2, for further displacements, the bending moment at the node A generally exceeds the cross-sectional elastic bending resistance and a second plastic hinge may develop [15]. Additionally, based on experimental observations and numerical results, it is assumed that the sheeting locally yields and the tie T_2 reaches its plastic resistance. Based on these assumptions, 3 degrees of freedom

are released. Hence, the degree of statical indeterminacy in the plastic stage is equal to:

$$n_{s,pl} = (5 + 31) - 3 \cdot 12 = 0 \tag{3}$$

Finally, under the conditions above, the analytical model in Figure 6 is stable and statically determinate.

3.2 Equilibrium equations

In consideration of the assumptions made, the statically determined system can be solved through equilibrium equations. However, in this contribution, the authors focus on the derivation of the load *P* without explicitly analysing the internal forces of the whole system.

Considering the bottom part of the stud (beam element) up to the point B, the horizontal equilibrium equation is given by:

$$V_B + P - T_2 + T_1 = 0 \tag{4}$$

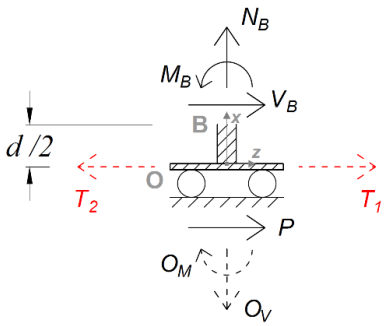

Figure 7 Internal forces and reaction forces acting on the bottom part OB of the stud (beam)

From Eq. (4), the shear force V_B can be written as:

$$V_B = T_2 - T_1 - P \tag{5}$$

According to the assumptions made, the bending moment at B is equal to the plastic bending resistance of the circular cross section M_{pl}.

$$M_B = +M_{pl} \tag{6}$$

with:

$$M_{pl} = \frac{f_u d^3}{6} \tag{7}$$

where f_u is the ultimate strength of the stud material.

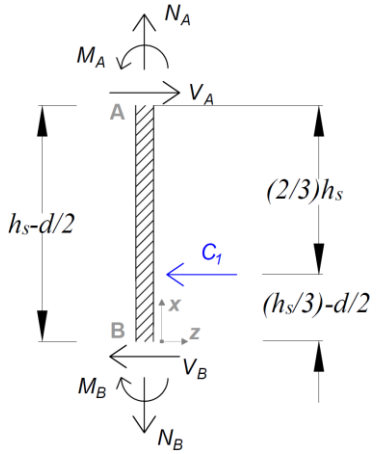

Figure 8 Internal forces and reaction forces of the segment AB of the stud (beam)

If the segment AB in Figure 8 is analysed, the rotational equilibrium equation around the node A delivers the following expression:

$$M_A - M_B - C_1 \cdot \frac{2}{3} h_s - V_B \cdot \left(h_s - \frac{d}{2}\right) = 0 \tag{8}$$

where the bending moment M_A is not necessarily equal to $-M_{pl}$. If the total number of plastic hinges developed in the stud is n_y, M_A is given by:

$$M_A = -(n_y - 1)\, M_{pl} \tag{9}$$

By substituting the expression of the internal forces V_B, M_A and M_B in Eq. (8), the resulting load *P* is equal to:

$$P = \frac{n_y M_{pl}}{h_s - d/2} + C_1 \cdot \frac{2h_s}{3(h_s - d/2)} + (T_2 - T_1) \tag{10}$$

Where:

$\frac{n_y M_{pl}}{h_s - d/2}$	is the bending component of the stud
$C_1 \frac{2h_s}{3(h_s - d/2)}$	is the concrete strut component
$(T_2 - T_1)$	is the steel sheeting component

As confirmed by Figure 3 and Figure 4, the resistance of the shear connector at post-cracking stage is mainly related to the local concrete crushing in front of the stud. Therefore, it is consistently assumed that the failure of the presented "modified strut and tie model" occurs when the strut C_1 reaches its capacity $C_{1,max}$:

$$P_R = P(C_1 = C_{1,max}) \tag{11}$$

All the members of the model proposed are considered as adequately ductile in order to exploit the resistance of the strut $C_{1,max}$ which is estimated in the next paragraph.

3.3 Resistance of strut $C_{1,max}$: analogy with RC corbel

The geometry of the rib in open-trough deck reminds the shape of reinforced concrete (RC) corbels. Such systems are usually well represented by a simple "strut and tie" model where the tension is taken by the reinforcement bars and the vertical load is transferred to the column through a diagonal concrete strut [12, 13]. The damage pattern in RC corbels is similar to what has been observed in the concrete rib at low displacements of headed stud shear connectors, see Figure 9.

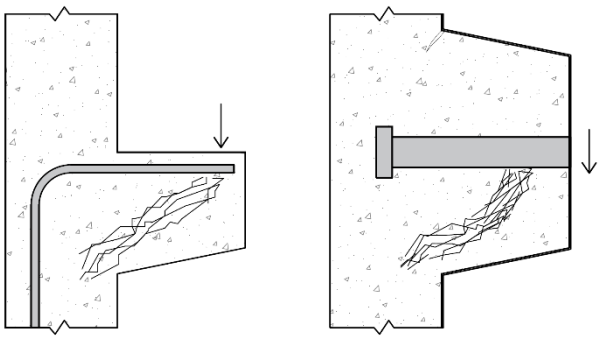

(a) (b)

Figure 9 Schematic of the concrete crack path (a) in RC corbel and (b) in the rib of headed stud shear connectors with profiled steel sheeting

Unlike in RC corbels, the concrete rib of the shear connection is enclosed by the steel sheeting. This provides an extra resistance component able to carry part of the load *P* through bending and tension. This justifies the fact that the orientation of the principal compressive stresses in the rib varies. Such effect is accounted in the model by means of the struts C_1 and C_{11} in Figure 10.

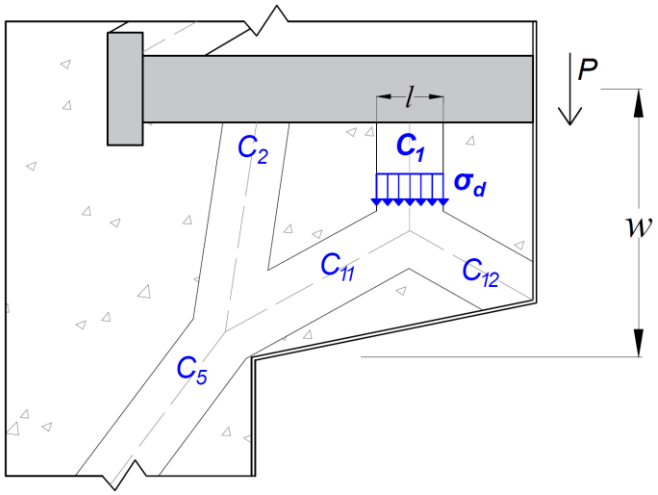

Figure 10 System of struts in front of the stud bas ed on the model in Figure 6

Due to the similarities of the damage pattern of the concrete rib with RC corbels, the authors use this analogy to estimate the resistance of the strut C_1. The force carried by this strut is equal to:

$$C_1 = \sigma_d \cdot l \cdot c \tag{12}$$

Where σ_d is the effective stress of the concrete strut, *l* is the width of the concrete (Figure 10) and *c* is the depth of the strut C_1.

The geometrical dimension *c* is assumed equal to *2d* as a result of the analysis of the compressive stresses observed in the FE model. However, further numerical investigations are recommended to calibrate this parameter more accurately. As assumed by Hwang et al. [13] for the "strut and tie" model of RC corbels, the effective width of the compressed strut *l* may be given by the depth to neutral axis of the cross section at the column interface and it is given by:

$$l = k \cdot w \tag{13}$$

With:

$$k = \sqrt{x^2 + 2x} - x \tag{14}$$

$$x = \frac{E_s}{E_{cm}} \frac{A_s}{cw} \tag{15}$$

Where A_s indicates the cross-sectional area of the headed stud.

The capacity of the strut C_1 is achieved when the effective compressive stress σ_d reaches its maximum value $\sigma_{d,max}$. In the strut and tie modelling, $\sigma_{d,max}$ is lower than the strength of the material in case of transversal tensile stresses that lead to longitudinal cracks, see Figure 11. With reference to the guidelines of EN 1992-1-1 for the design of RC corbel [17], the maximum stress of the cracked strut C_1 is taken as 0.6 f_c.

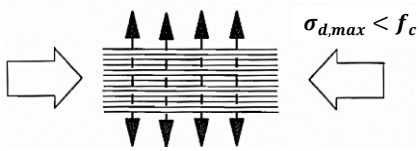

Figure 11 Compressive strength of the concrete strut with longitudinal cracks [17]

Therefore, the expression of the maximum load carried $C_{1,max}$ by the strut is given by:

$$C_{1,max} = 0.6 f_c \cdot k \cdot w \cdot 2d \tag{16}$$

3.4 Number and position of the plastic hinges in the stud

Because of the difficulty in evaluating the stresses in the studs embedded in the concrete during the tests, a finite element model was developed. A stress-based method was used to estimate the degree of activation of the yield hinges, namely "number of plastic hinges" n_y [15]. First, the cross-sectional normal stresses σ_N were extracted from the path nodes at the level of the "plastic hinge", see Figure 12.

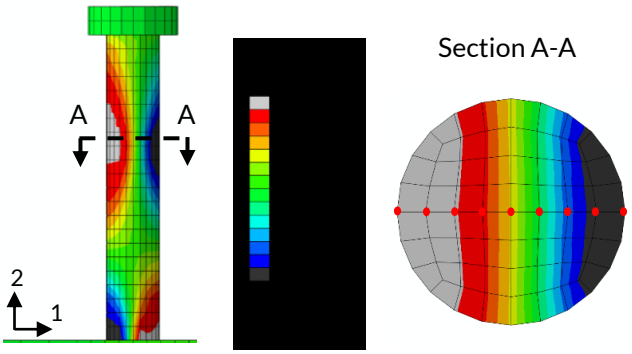

(a) (b)

Figure 12 Normal stress (S22) contour of the headed stud: (a) side and (b) cross-sectional view at the height of the upper yield hinge (section A-A) with the relative path nodes [15].

Then, with reference to Figure 13, the application of the equilibrium equation around the local axis *y* gives the bending moment M_y in Eq.(17) where the stress function $\sigma_N(x)$ was taken as a piecewise liner function.

$$M_y = \int_A [\sigma_N(x) \cdot x] dA = \int_{-\frac{d}{2}}^{\frac{d}{2}} [\sigma_N(x) \cdot b(x) \cdot x] dx \tag{17}$$

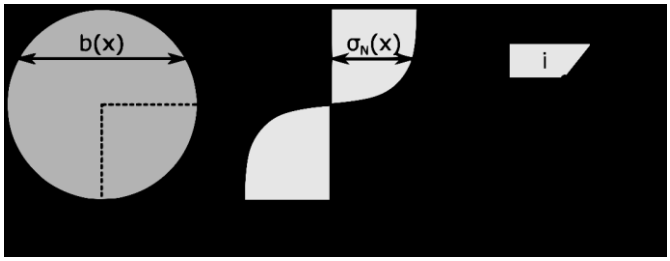

Figure 13 Real and numerical discrete normal stress distribution along the cross-section of the stud [15]

Finally, the value of M_y was compared with the full plastic resistance capacity M_{pl} defined in Eq.(7). Assuming that one plastic hinge always develops at the base of the shank, the resulting activated plastic hinges n_y is:

$$n_y = 1 + \frac{M_y}{M_{Pl}} \leq 2 \tag{18}$$

Based on the numerically obtained values of n_y at a slip of 4 mm, the analytical function is proposed in Eq. (19) and plotted in Figure 14 for n_r=2 as a function of the normalized embedment length h_A/d.

$$n_y = \begin{cases} 2 & \text{for } n_r = 1 \text{ or staggered position} \\ 1.67\frac{h_A}{2d} - 0.17 \le 2\text{, but not less than 1} & \text{for } n_r = 2 \end{cases} \quad (19)$$

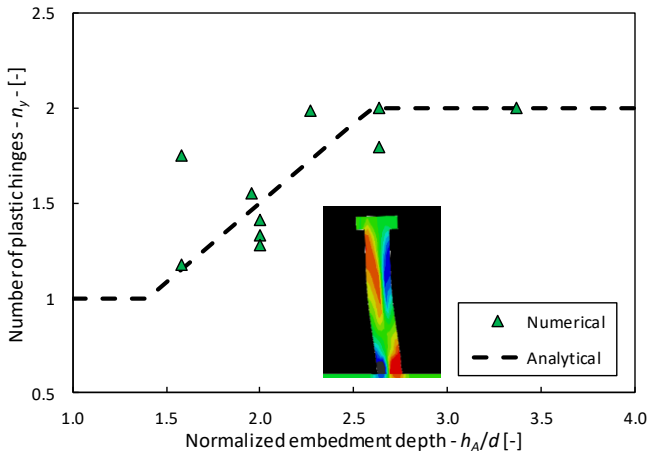

Figure 14 Comparison between numerically obtained and analytical values of the number of plastic hinges n_y for two studs per rib (n_r=2) at a slip of 4 mm

From the same numerical study, the vertical position of the upper hinge h_s was also extracted. The following simplified expression of h_s is given by:

$$h_s = (0.4n_r + 0.2)\frac{120 \cdot h_p}{b_0}\text{[mm]} \le h_p\text{, but not less than } 2d \quad (20)$$

Where b_0 is the mean width of the rib, see Figure 15. Due to the reduced scope of the numerical study, it is recommended to perform further investigations to ensure the reliability of Eq. (20).

3.5 Correction factors

In case of two studs placed in the same rib, part of the concrete is subjected to higher stresses due to their interaction. A reduction factor k_n=0.8 applied to $C_{1,max}$ is proposed when 2 studs are placed in the stud.

The component of the load taken by the deck steel deck in Eq. (10) is simplified as follows:

$$T_2 - T_1 = k_w \cdot f_{yp}\pi t d \quad (21)$$

Where f_{yp} is the yield strength of the material of the steel deck and t indicates its thickness. From a statistical evaluation of different subsets, a reduction factor k_w=0.6 is introduced for pre-punched hole configurations whereas no reduction is considered for through-deck welded studs (i.e. k_w=1.0).

3.6 Proposed equation

Based on the procedure described in the previous paragraphs, the final proposed expression for predicting the post-cracking resistance P_R of the headed stud connector in profiled steel sheeting is summarized in Eq. (22).

As none of the reported push-out tests on headed studs with profiled sheeting exhibits premature shear failure of the stud shank within the first 6 mm of slip, no upper bound for shear failure was considered. Hence, only one resistance equation is given.

$$P_R = k_n(1.2f_c \cdot d \cdot k \cdot w) \cdot \zeta + \frac{n_y f_u d^3/6}{h_s - d/2} + k_w \cdot f_{yp}\pi t d \quad (22)$$

With:

$$k_n = \begin{cases} 1.0 & \text{for } n_r = 1 \\ 0.8 & \text{for } n_r = 2 \end{cases} \quad (23)$$

$$k = \sqrt{x^2 + 2x} - x \quad (24)$$

$$x = \frac{E_s}{E_{cm}}\frac{\pi d}{8w} \quad (25)$$

$$\zeta = \frac{2}{3}\left(\frac{h_s}{h_s - 0.5d}\right) \quad (26)$$

$$n_y = \begin{cases} 2 & \text{for } n_r = 1 \text{ or staggered position} \\ 1.67\frac{h_A}{2d} - 0.17 \le 2\text{, but not less than 1} & \text{otherwise} \end{cases} \quad (27)$$

$$h_s = (0.4n_r + 0.2)\frac{120 \cdot h_p}{b_0}\text{[mm]} \le h_p\text{, but not less than } 2d \quad (28)$$

$$k_w = \begin{cases} 1.0 & \text{for through} - \text{deck welding studs} \\ 0.6 & \text{for pre} - \text{punched hole sheeting} \end{cases} \quad (29)$$

Where:

E_{cm} is the secant modulus of elasticity of the concrete

E_s is the modulus of elasticity of the stud material

f_c is the compressive strength of the concrete

f_u is the ultimate tensile strength of the stud material

f_{yp} is the yield strength of the material of the sheeting

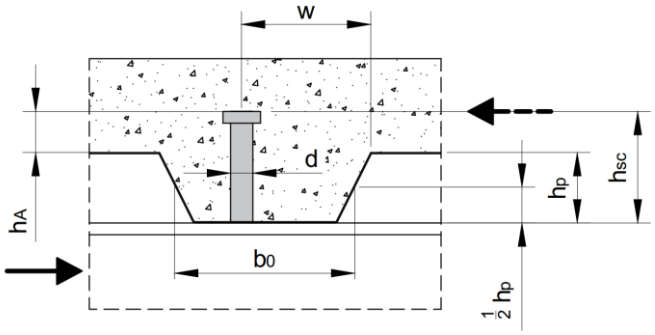

Figure 15 Geometrical properties of headed shear connector in open trough decks

4 Comparison with experimental results

To assess whether the analytical resistance in Eq. (22) predicts well the experimental resistance of the shear connector, a test database of more than 300 push-out tests with studs welded in open trough profiled decks is initially considered. In consideration of the field of application of current design EN 1994-1-1 rules, the following requirements shall be fulfilled:

- Number of studs per rib n_r are not more than 2
- No transversal load is applied to the concrete slabs due to its influence on the resistance [18]
- No tests with weld seam failure
- The estimated characteristic concrete cylinder strength f_{ck} according to EN 1992-1-1 [17] is not lower than 17 N/mm².

193 push-out tests satisfy the conditions above. In order to compare experimental and analytical values in a consistent manner, the mean mechanical and geometrical properties are used in the calculation of the resistance P_R. All the mean values are based on the measured values provided in each test. If the geometrical dimensions were not measured, the mean values were calculated from the nominal values. The comparison between the experimental and analytical values of the resistance is shown in Figure 16.

The linear correlation factor R=0.807 confirms that the derived resistance function predicts well the actual resistance of the shear connectors. On the other side, the scattering of the results is given by the coefficient of variation V which is equal to 0.149.

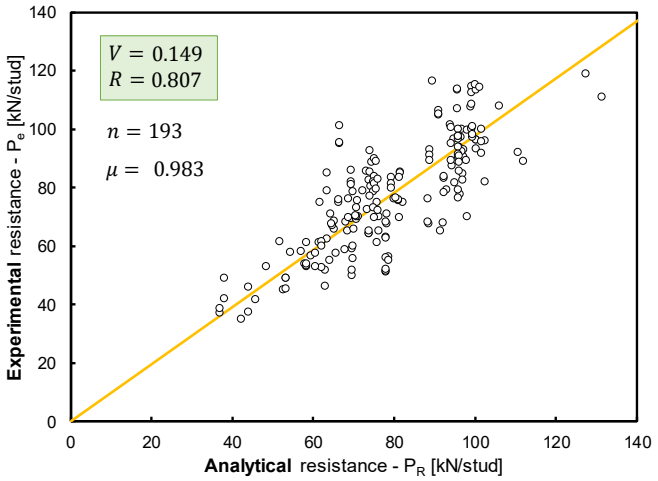

Figure 16 Comparison between the analytical resistance P_R of Eq.(22) and the experimental strength P_e from 193 push-out tests

As suggested in EN 1990 Annex D [19] procedure, the resistance function was also evaluated against different subsets.

Table **1** shows that the prediction of the resistance delivers better results for studs placed in centred position compared to the cases with studs placed on the unfavourable or favourable side of the trough. This may be due to the lack of information on the bending component carried by the studs (i.e. values of n_y and h_s). From the results displayed in Table 2 , the effect of the stud number as well as the type of welding is properly considered in the model. Notwithstanding that, a more refined approach for cases with 2 studs per trough is recommended.

Table 1 Mean μ and coefficient of variation V of P_e/P_R for all cases and for different eccentrical position of the stud

P_e/P_R	All	Centred Position	Favourable Position	Unfavourable Position	Staggered Position
N	193	112	36	28	17
μ	0.983	1.003	0.903	0.996	0.997
V	0.149	0.111	0.197	0.194	0.145

Table 2 Mean μ and coefficient of variation V of P_e/P_R for different subsets

P_e/P_R	n_r=1	n_r=2	Pre-punched holes	Through-deck welding
n	141	52	56	137
μ	1.013	0.901	1.018	0.968
V	0.135	0.158	0.120	0.158

5 Conclusions

In view of the results presented in this study, the following conclusions can be drawn:

- The damage pattern observed in tests was used to define the sequence resistance mechanisms of headed stud shear connectors in profiled decks at low displacements.
- With the additional support of a FE model, a "modified strut and tie model" was developed. The concrete rib was modelled through struts, the steel deck was replaced by tension ties and the stud was considered as a beam element (tension and bending moment). This system describes the mechanical behaviour in the post-cracking stage (i.e. after initiation of concrete cone failure) at a slip displacement of around 2-6 mm.
- In the elastic stage, the analytical model proposed is 3 times statically indeterminate. Considering both the plastic hinges in the studs and the yielding of the tension tie T_2 (pulling force of the sheeting), it becomes statically determinate and the equilibrium equations are sufficient to solve the structure.
- The analogy between the concrete rib of the shear connection and RC corbels was used to estimate the resistance of the concrete strut $C_{1,max}$. The number and position of the plastic hinges in the stud were evaluated through numerically obtained values whereas the correction factors accounting for the welding type and the number of studs per trough were statically determined.
- By comparing the resulting analytical post-cracking resistance P_R with the experimental push-out test results, a good agreement is found: the coefficient of variation V is 0.149 while the linear correlation coefficient is 0.807.

Acknowledgements

The authors of this article gratefully acknowledge the financial support of ArcelorMittal Global R&D, Long Products, Luxembourg, for promoting the work presented within the scope of the "ShearCON" research project under grant number UL-E-AGR-0022-10-C.

References

[1] British Standards Institution (2004) *EN 1994-1-1. Eurocode 4 - Design of composite steel and concrete structures Part 1-1: General rules and rules for buildings.* London: BSI.

[2] Lloyd, R.; Wright, H. D. (1990) *Shear connection between composite slabs and steel beams*. Journal of constructional steel research **15**, H. 4, S. 255-285.

[3] Lawson, M.; Aggelopoulos, E.; Obiala, R.; Hanus, F.; Odenbreit, C.; Nellinger, S.; Kuhlmann, U.; Eggert, F.; Lam, D.; Dai, X.; Sheehan, T. (2017) *Development of improved shear connection rules in composite beams - Final Report*.

[4] Konrad, M. (2011) *Tragverhalten von Kopfbolzen in Verbundträgern bei senkrecht spannenden Trapezprofilblechen*. PhD Dissertation. Stuttgart: Institut für Konstruktion und Entwurf, Stahl- Holz- und Verbundbau, Universität Stuttgart.

[5] Odenbreit, C.; Vigneri, V.; Amadio, C.; Bedon, C.; Braun, M. (2018) *New mechanical model to predict the load bearing resistance of shear connectors with modern forms of profiled sheeting.* 13th International Conference on Steel, Space and Composite Structures. Perth.

[6] Nellinger, S. (2015) *On the behaviour of shear stud connections in composite beams with deep decking*. Ph.D. Dissertation. Luxembourg: University of Luxembourg.

[7] Vigneri, V.; Odenbreit C.; Lam, D. (2019) *Different load bearing mechanisms in headed stud shear connectors for composite beams with profiled steel sheeting*. Steel Construction **12**, H. 3, S. 184-190.

[8] Jenisch, F. M. (2000) *Einlüsse des profilierten Betongurtes und der Querbiegung auf das Tragverhalten von Verbundträgern*. Ph.D. Dissertation. Kaiserslautern: Technische Universität Kaiserslautern.

[9] Bode, H.; Künzel, R. (1991) *Zur Anwendung der Durchschweisstechnik im Verbundbau 2/91*," Kaiserslautern.

[10] Johnson, R. P.; Yuan, H. (1998) *Models and design rules for stud shear connectors in troughs of profiled sheeting*. Proceedings of the Institution of Civil Engineers - Structures and Buildings **128**, H. 3, S. 252-263.

[11] Ernst, S. (2006) *Factors affecting the behaviour of the shear connection of steel-concrete composite beams*. Ph.D. Dissertation. Sidney: University of Western Sydney.

[12] Russo, G.; Venir, R.; Pauletta M.; Somma, G. (2006) *Reinforced Concrete Corbels — Shear Strength Model and Design Formula*, ACI Structura Journal **103**, H. 1, S. 3-10.

[13] Hwang, S. J.; Lu W. Y.; Lee, H. J. (2000) *Shear Strength Prediction for Reinforced Concrete Corbels*, ACI Strucutral Journal **97**, H. 4, S. 543-552.

[14] Lungershausen, H. (1988) *Zur Schubtragfähigkeit von Kopfbolzendübeln*. Ph.D. Dissertation. Bochum: Ruhr Universität Bochum.

[15] Vigneri, V.; Odenbreit, C.; Braun, M. (2019) *Numerical evaluation of the plastic hinges developed in headed stud shear connectors in composite beams with profiled steel sheeting*. Structures **21**, S. 103-110.

[16] Shen, M. H.; Chung, F. F. (2017) *Structural behaviour of stud shear connections with solid and composite slabs under co-existing shear and tension forces*. Structures **9**, S. 79-90.

[17] British Standards Institution (2004) *EN 1994-1-1. Eurocode 2 - Design of concrete structures Part 1-1: General rules and rules for buildings.* London: BSI.

[18] Nellinger, S.; Odenbreit, C.; Obiala R.; Lawson, M. (2017) *Influence of transverse loading onto push-out tests with deep steel decking*. Journal of Constructional Steel Research **128**, S. 335-353.

[19] British Standards Institution (2002) *EN 1990. Eurocode – Basis of stuctural design.* London: BSI.